Pure Appl. Chem., Vol. 74, No. 9, pp. 1571–1580, 2002.

Organometallic precursor route to carbon nanotubes*

A. Govindaraj and C. N. R. Rao‡

Chemistry and Physics of Materials Unit and CSIR Center of Excellence in Chemistry, Jawaharlal Nehru Centre for Advanced Scientific Research, Jakkur P.O., Bangalore 560 064, India

Abstract: Multi-walled as well as single-walled carbon nanotubes are conveniently prepared by the pyrolysis of organometallic precursors, such as metallocenes and phthalocyanines, in a reducing atmosphere. Pyrolysis of organometallics alone or in mixture with hydrocarbons also yields aligned nanotube bundles with useful field emission properties. By pyrolyzing organometallics in the presence of thiophene, Y-junction nanotubes are obtained in large quantities. The junction nanotubes have a good potential in nanoelectronics. Carbon nanotubes prepared from organometallics are useful for preparing nanowires and nanotubes of materials such as BN, GaN, SiC, and Si_3N_4.

INTRODUCTION

Carbon nanotubes were first found in the cathode deposits obtained in the arc evaporation of graphite [1]. The arc method has since been employed to obtain good yields of both multi- and single-walled nanotubes (MWNTs and SWNTs). Carbon nanotubes are also obtained by carrying out the pyrolysis of hydrocarbons over nanoparticles of iron, cobalt, and other metals dispersed over a solid substrate [2–4]. The presence of nanoparticles is essential for the formation of the nanotubes and to control the diameter of the nanotube to some extent [5]. Since a carbon source, as well as metal nanoparticles, is necessary for producing carbon nanotubes by the pyrolysis of hydrocarbons, we have employed organometallic precursors that can serve as a dual source of both the carbon and the metal nanoparticles. Our early experiments on the pyrolysis of metallocenes were successful in producing MWNTs [6,7]. We have employed this method to produce MWNTs and SWNTs as well as to make aligned nanotube bundles and Y-junction nanotubes. In this article, we present the salient features of the various types of nanotubes obtained by employing the organometallic route.

MULTI- AND SINGLE-WALLED NANOTUBES

MWNTs and metal-filled, onion-like structures were prepared by the pyrolysis of metallocenes such as ferrocene, cobaltocene, and nickelocene under reducing conditions, wherein the precursor acts as the source of the metal as well as carbon [6]. The pyrolysis set-up consists of stainless steel gas-flow lines and a two-stage furnace system fitted with a quartz tube (25-mm inner diameter) as shown in Fig. 1a, the flow rate of the gases being controlled by the use of mass flow controllers. In a typical preparation, a known quantity (100 mg) of the metallocene (presublimed 99.99 % purity) is taken in a quartz boat and placed at the center of the first furnace, and a mixture of Ar and H_2 of the desired composition

Pure Appl. Chem.* **74, 1489–1783 (2002). An issue of reviews and research papers based on lectures presented at the 2nd IUPAC Workshop on Advanced Materials (WAM II), Bangalore, India, 13–16 February 2002, on the theme of nanostructured advanced materials.

‡Corresponding author: Fax: 91-80-8462760; E-mail: cnrrao@jncasr.ac.in.

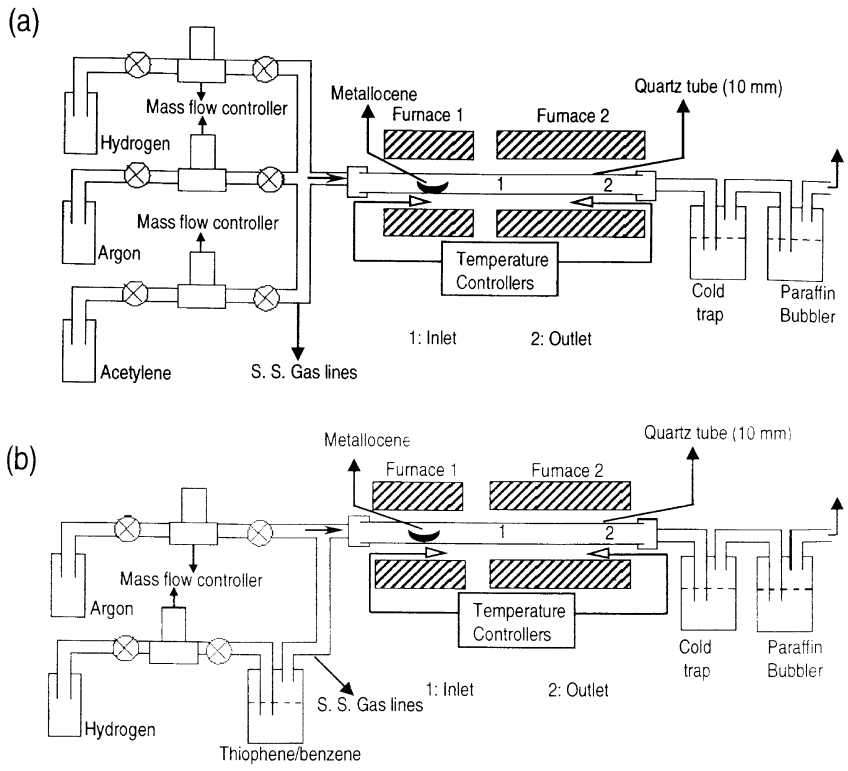

Fig. 1 Pyrolysis apparatus employed for the synthesis of carbon nanotubes by pyrolysis of mixtures of (a) metallocene + C_2H_2 and (b) metallocene + benzene or thiophene. The numbers 1 and 2 indicated in the figure represent inlet and outlet, respectively.

passed through the quartz tube. The metallocene is sublimed by raising the temperature of the first furnace to 200 °C at a controlled heating rate (20 °C/min). The metallocene vapor so generated is carried by the Ar–H_2 gas stream into the second furnace, maintained at 900 °C where the pyrolysis occurs, yielding large quantities of carbon deposits, mainly containing carbon nanotubes. These deposits are examined by a scanning electron microscope (SEM) and transmission electron microscope (TEM). To increase the yield of the MWNTs with metallocene, vapors of an additional hydrocarbon source were mixed along with the metallocene vapor in the first furnace. Thus, pyrolysis of benzene or C_2H_2 in the presence of ferrocene gives high yields of MWNTs, the wall thickness of the nanotubes depending on the proportion of the carbon source and the metal precursor [7]. In Fig. 2a, we show a TEM image of nanotubes obtained by the pyrolysis of a mixture of C_2H_2 (25 sccm) and ferrocene at 1100 °C in an Ar flow rate of 1000 sccm (sccm = standard cubic centimeter per minute). The image clearly reveals that the addition of hydrocarbon not only increases the yield of hollow MWNTs, but also reduces the amount of carbon-coated metal nanoparticles. In Fig. 2b, we show a TEM image of MWNTs obtained by the pyrolysis of a mixture of nickelocene and benzene at 900 °C in 85 % Ar and 15 % H_2 mixture at a flow rate of 1000 sccm. Besides metallocenes, one can also employ metal phthalocyanines as precursors to prepare MWNTs [8,9].

In order to prepare SWNTs, alternate synthetic strategies have been explored. Under controlled conditions of pyrolysis, dilute hydrocarbon-organometallic mixtures yield SWNTs [10,11]. High-resolution TEM images of SWNTs, obtained by the pyrolysis of a nickelocene–acetylene mixture at 1100 °C, [11] is shown in Fig. 2c. The diameter of the SWNT in Fig. 2c is 1.4 nm. Pyrolysis of cobaltocene and acetylene under similar conditions gives rise to isolated SWNTs. In Fig. 2d, we show the

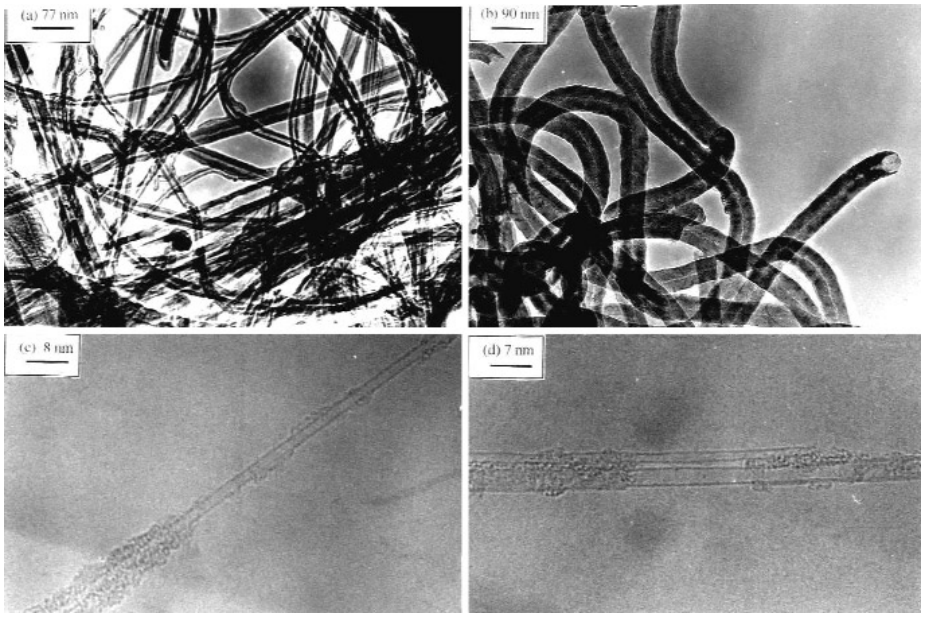

Fig. 2 (a) TEM image of an MWNT obtained by pyrolysis of a mixture of C_2H_2 (25 sccm) and ferrocene at 1100 °C at 1000 sccm Ar flow. (b) TEM image of an MWNT obtained by pyrolysis of a mixture of nickelocene and benzene at 900 °C in 85 % Ar and 15 % H_2 mixture at a flow rate of 1000 sccm. (c) HREM image of SWNTs obtained by the pyrolysis of nickelocene and C_2H_2 at 1100 °C in a flow of Ar (1000 sccm) with C_2H_2 flow rate of 50 sccm. (d) HREM image of SWNTs obtained by the pyrolysis of ferrocene and CH_4 at 1100 °C in a flow of Ar (990 sccm) with CH_4 flow rate of 10 sccm.

high-resolution electron microscope (HREM) images of the SWNTs obtained by the pyrolysis of ferrocene with methane at 1100 °C. Pyrolysis of binary mixtures (1:1 by weight) of the metallocenes along with acetylene gives good yields of SWNTs, owing to the beneficial effect of binary alloys [12]. Pyrolysis of ferrocene–thiophene mixtures yield SWNTs, but the yield is somewhat low. Pyrolysis of a mixture of benzene and thiophene along with ferrocene (Fig. 1b), however, gives a high yield of SWNTs [13].

TEM examination of the various carbonaceous products obtained from the pyrolysis of hydrocarbons and organometallic precursors indicates that the size of the catalyst particle plays an important role, with regard to the nature of the product. In the case of organometallic precursors, it seems that metal nanoclusters of ~1-nm diameter are produced under controlled conditions. When the concentration of the organometallic precursor is high, MWNTs are formed around the metal particles of 5–20-nm diameter. This is true of carbon nanotubes obtained by the metallocene route [6,7]. In the higher size range of ≥50 nm, graphite-covered metal particles are formed predominantly [14].

ALIGNED CARBON NANOTUBE BUNDLES

Since the pyrolysis of mixtures of organometallic precursors and hydrocarbons yields good quantities of MWNTs [6,7], we considered the possibility of obtaining aligned nanotube bundles under appropriate conditions. For this purpose, we carried out pyrolysis of metallocenes along with other hydrocarbon sources, in the apparatus shown in Fig. 1a [10,15,16]. In order to obtain aligned nanotube bundles, a typical heating rate 50 °C/min of the first furnace and an Ar flow rate of 1000 sccm have been employed. Compact aligned nanotube bundles could be obtained by introducing C_2H_2 (50–100 sccm)

during the sublimation of ferrocene. SEMs of aligned nanotubes obtained by the pyrolysis of ferrocene are shown in Figs. 3a–3c. The image in Fig. 3a shows larger bundles of aligned nanotubes. The image in Fig. 3b shows the side view, and the image in Fig. 3c shows the top view of the aligned nanotubes, wherein the nanotube tips are seen. The average length of the nanotubes is generally around 60 μm with methane and acetylene. In the case of methane, the nanotubes are aligned, but the packing density is not high. The nanotube bundles obtained with ferrocene + acetylene mixtures appear to have a packing density greater than that obtained with Fe/silica catalysts [17]. TEM image of a part of an aligned nanotube bundle obtained from the pyrolysis of the acetylene–ferrocene mixture is shown in Fig. 3d. A small proportion of graphite-covered metal nanoparticles is often present along with the nanotubes. Considering all aspects, we feel that the pyrolysis of organometallic precursors is the most convenient means of preparing aligned MWNTs. The advantage of the precursor method is that the aligned bundles are produced in one step, at a relatively low cost, without prior preparation of substrates. The metal often gets encapsulated to form nanorods or nanoparticles inside the carbon nanotubes. Ferromagnetism of these metal particles is also a property of significance. The iron nanorods encapsulated in the nanotubes exhibit a complex behavior with respect to magnetization reversal and could be useful as probes in magnetic force microscopy.

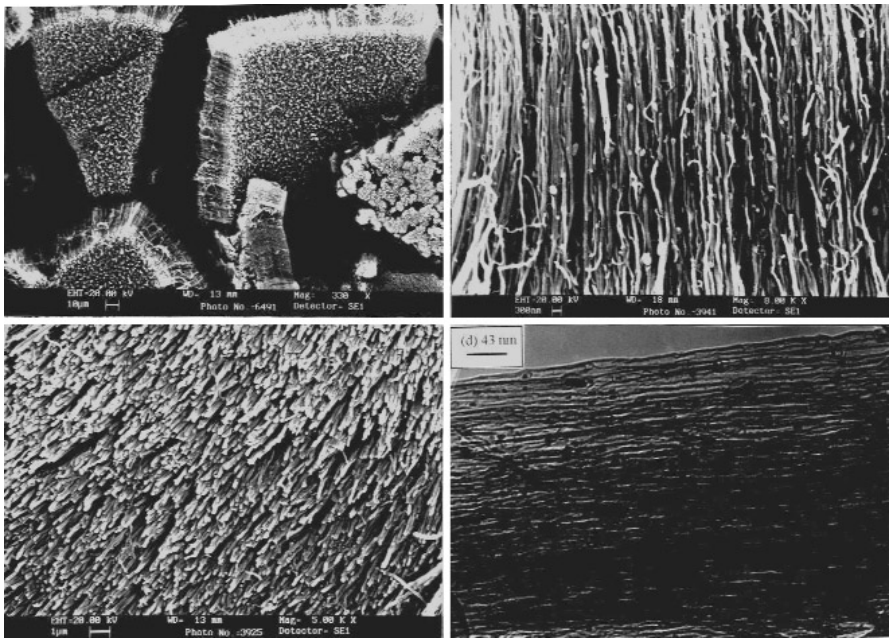

Fig. 3 SEM image (a) showing the bundles of aligned nanotubes obtained by pyrolyzing ferrocene along with butane (50 sccm) at 1100 °C in an Ar flow of 950 sccm. (b) and (c) show views of the aligned nanotubes perpendicular to and along the axis of the nanotubes, respectively. (d) TEM image of a part of an aligned nanotube bundle obtained from the pyrolysis of acetylene (85 sccm) and ferrocene mixture at 1100 °C in an Ar flow of 1000 sccm.

Y-JUNCTION CARBON NANOTUBES

Device miniaturization in semiconductor technology is expected to reach its limits owing to the inherent quantum effects as one goes towards smaller size. In such a scenario, an alternative would be nanoelectronics based on molecules. The possible use of carbon nanotubes in nanoelectronics has aroused

considerable interest. For such applications, it is important to be able to connect the nanotubes of different diameters and chirality [18–20]. Complex three-point nanotube junctions have been proposed as the building blocks of nanoelectronics, and in this regard, Y- and T-junctions have been considered as prototypes [21,22]. While we would expect an equal number of five- and seven-membered rings to create nanotube junctions, it appears that they can be created with an equal number of five- and eight-membered rings as well [22]. However, junctions consisting of crossed nanotubes have been fabricated to study their transport characteristics [23]. Y-junction nanotubes have been produced by using Y-shaped nanochannel alumina as templates [24]. We have prepared Y-junction nanotubes in large quantities by carrying out the pyrolysis of a mixture of a metallocene with thiophene [25,26].

The experimental set-up we used for the synthesis of the Y-junction nanotubes employed a two-stage furnace system similar to that described earlier (Fig. 1b) [25]. A known quantity of metallocene was sublimed in the first furnace and carried along with a flow of argon (Ar) gas to the pyrolysis zone in the second furnace. Simultaneously, hydrogen was bubbled through thiophene and was mixed with the argon-metallocene vapors at the inlet of the furnace and carried to the pyrolysis zone. Pyrolyzing the mixed vapors at 1000 °C yielded Y-junction nanotubes in plenty. Pyrolysis of Ni/Fe phthalocyanine in mixture with thiophene was carried out in a similar manner, taking phthalocyanine in place of the metallocenes to obtain good Y-junction nanotubes. Pyrolysis of various organometallics with sulfur-containing compounds has shown that pyrolysis of thiophene with nickelocene, ferrocene, and cobaltocene yields excellent Y-junction nanotubes. A low-magnification TEM image revealing the presence of several Y-junction carbon nanotubes obtained by the pyrolysis of nickelocene/thiophene mixture is shown in Fig. 4a. Many of the nanotubes show multiple Y-junctions. A TEM image of a single long Y-junction nanotube is shown in Fig. 4b.

Pyrolysis of thiophene with Fe- or Ni-phthalocyanine or iron pentacarbonyl also yields Y-junction nanotubes. In Fig. 4c, we show few Y-junctions, whereas in Fig. 4d, we show the multiple junc-

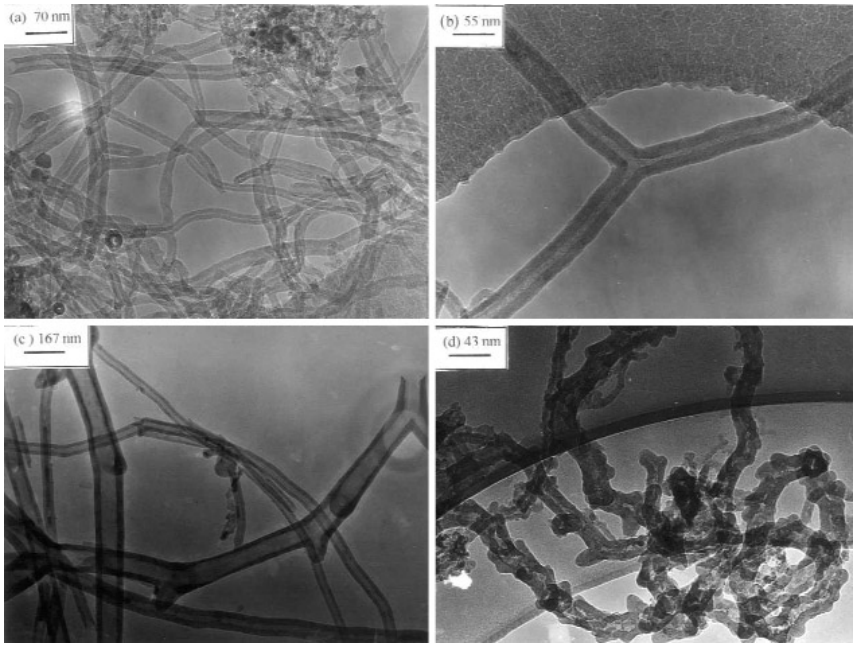

Fig. 4 (a),(b) TEM images of Y-junction carbon nanotubes obtained by the pyrolysis of nickelocene and thiophene at 1000 °C. (c),(d) TEM images of Y-junction nanotubes obtained by the pyrolysis of thiophene along with Ni-phthalocyanine at 1000 °C.

tions formed continuously by the pyrolysis of thiophene with Ni-phthalocyanine. While the pyrolysis of nickelocene with CS_2 yields similar junctions, the yield and quality of the nanotubes is not satisfactory. Compositional analysis at the Y-junction has shown absence of sulfur, indicating that the junction is formed by the curvature caused by different carbon rings. The metal nanoparticles abstract the sulfur from thiophene, forming a sulfide, the remaining carbon fragment probably being involved in ring formation.

HREM images show that the graphitic layers bend in parallel with respect to the junction in many of these nanotubes. Our studies in collaboration with Torsteen Seeger and Manfred Rühle have shown that the Y-juction tubes are entirely composed of carbon with no sulfur impurity. These observations suggest the presence of equal numbers of five- and seven-/eight-membered rings at the junctions. The metal particles formed in the pyrolysis contain both sulfur and carbon.

Scanning tunneling spectroscopic studies of Y-junction carbon nanotubes show interesting diode-like device characteristics at the junctions. A typical I-V curve obtained from positioning the tip atop a Y-junction (the point of contact between the three arms) is asymmetric with respect to bias polarity, unlike that along the arm or on the individual arms of the Y-junction. The plot of differential conductance vs. bias with respect to zero bias is symmetric along the arm and asymmetric at the junctions. Such asymmetry is characteristic of a junction diode, and this in turn indicates the existence of intramolecular junctions in the carbon nanotubes. The findings discussed above open up the possibility of assembling carbon nanotubes possessing novel device-like properties [25,27–29] into multifunctional circuits, and ultimately towards the realization of a carbon nanotube-based computer chip.

NANORODS, NANOWIRES, AND NANOTUBES OF OTHER MATERIALS

Preparation of metal nanorods covered by carbon has been reported in the recent literature [10,30–32]. The organometallic precursor route provides a means of preparing metal nanorods. The pyrolysis of ferrocene + hydrocarbon mixtures or of ferrocene alone yields iron nanorods encapsulated inside the carbon nanotubes as evidenced from TEM, the proportion of the nanorods depending on the proportion of ferrocene. Typical TEM images of such nanorods are shown in Figs. 5a and 5b. The selected area electron diffraction (SAED) pattern of the nanorods shows spots due to (010) and (011) planes of α-Fe. The HREM image of the iron nanorod in Fig. 5c shows well-resolved (011) planes of α-Fe in single-crystalline form. Ni/Fe phthalocyanines can be used in the place of metallocenes to prepare metal nanowires. However, the yields are not as good as in the case of metallocenes.

There are several reports on the preparation of SiC nanowires in the literature, but fewer on the preparation of Si_3N_4 nanowires [33,34]. The methods employed for the synthesis of SiC nanowires have been varied. Since both SiC and Si_3N_4 are products of the carbothermal reduction of SiO_2, it should be possible to establish conditions wherein one set of specific conditions favor one over the other. We have been able to prepare Si_3N_4 nanowires [35], by reacting MWNTs produced by ferrocene pyrolysis with ammonia and silica gel at 1360 °C. The MWNTs were used as a carbon source in the carbothermal reduction because they have higher thermal stability compared to activated carbon. The reaction of aligned MWNTs (produced by metallocene route) with silica gel and NH_3 at 1360 °C yields a mixture of α- and β-Si_3N_4. SEM images of the product obtained by this reaction showed the nanowires to have large diameters (5–7 micron), with lengths of the order of hundreds of microns (Fig. 6). By addition of catalytic iron particles (0.5 atom %), we obtain β-SiC nanowires under the same conditions (Fig. 6b) [35]. In Fig. 5d, we show an HREM image of a single crystalline β-SiC nanowire so obtained.

Several chemical methods of preparing boron nitride nanotubes and nanowires have been investigated [36]. The general methods involve reacting boric acid with ammonia in the presence of MWNTs. Aligned BN nanotubes are obtained by heating aligned bundles of MWNTs with boric acid in the presence of ammonia at 1000–1300 °C range. The SEM images of aligned BN nanotube bundles are shown in Fig. 6c. The average outer diameter of the aligned BN nanotubes varies from 15 to 40 nm as revealed by the TEM image in Fig. 6d. This suggests that during the formation of BN nanotubes, the

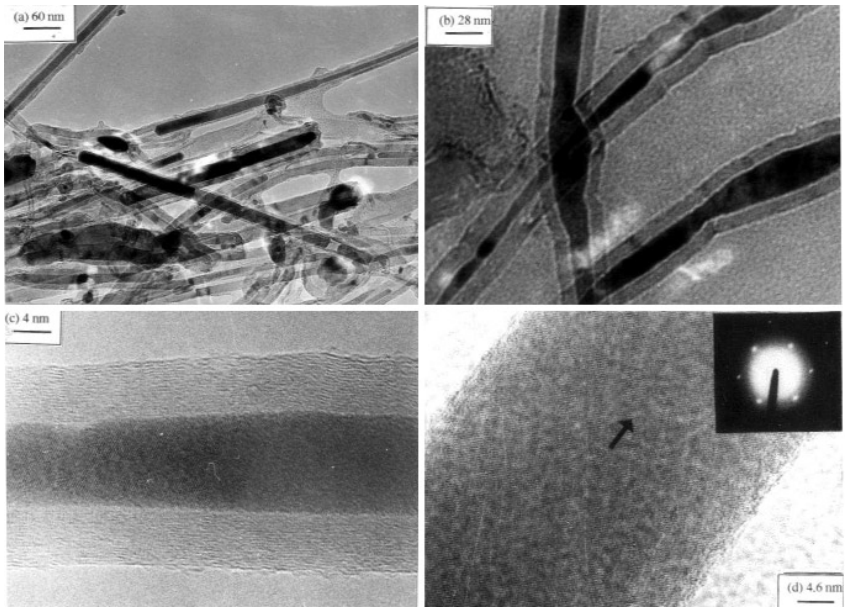

Fig. 5 (a), (b) TEM images of the iron nanorods/nanowires encapsulated inside the carbon nanotubes from aligned nanotube bundles. (c) HREM image of a single crystal iron nanowire encapsulated inside a carbon nanotube. (d) HREM image of a SiC nanowire prepared by heating silica gel containing aligned bundles of MWNTs for 7 h at 1360 °C. The inset shows the SAED pattern. The arrow denotes the normal to the (111) planes and the direction of growth of the nanowire.

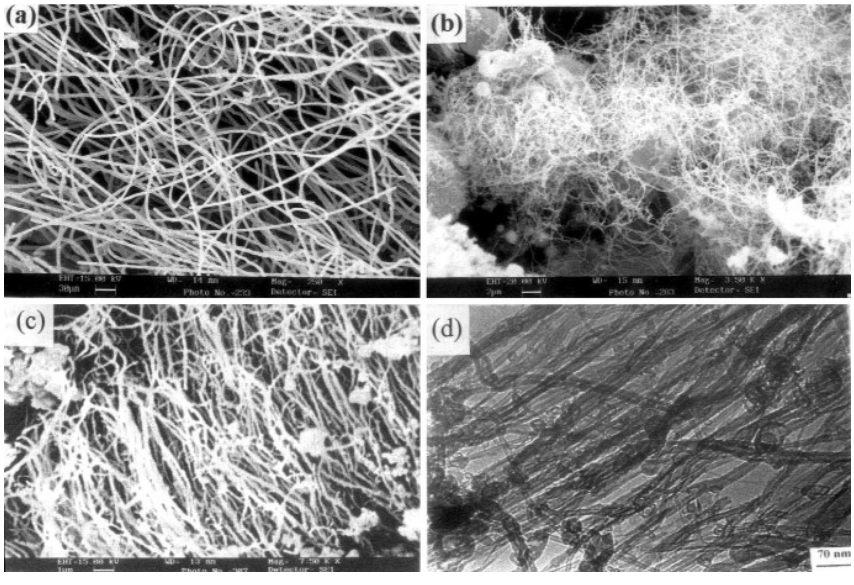

Fig. 6 (a) SEM image of Si_3N_4 nanowires obtained by the reaction of aligned MWNTs (produced by metallocene route) with silica gel at 1360 °C. (b) SiC nanowires. (c) SEM image of BN nanotubes obtained by heating aligned bundles of MWNTs with boric acid in the presence of ammonia at 1300 °C. (d) TEM image of the BN nanotubes obtained by the same procedure as in (a) and (b).

carbon MWNTs not only take part in the reaction, but also serve as templates. It is noteworthy that the BN nanotubes can be produced at a temperature as low as 1000 °C by this procedure. Based on elemental analysis and X-ray diffraction, it is found that the carbon content of the BN nanotubes becomes marginal if the initial proportion of carbon nanotubes is kept low.

We have prepared gallium nitride nanowires by employing several procedures involving the use of carbon nanotube templates [37]. We have employed gallium acetylacetonate as the precursor for the in situ production of small particles of the oxide (GaO_x), which then react with NH_3 vapor around 900 °C in the presence of nanotubes. The length of the nanowires extends to a few microns. The linear nanowires are generally single crystalline, showing a layer spacing of 0.276 nm corresponding to the [100] planes. The growth direction of the nanowires is nearly perpendicular to the [100] planes. The diameter of the nanowires is around 35–100 nm range and could be reduced to 20 nm by using SWNTs in place of MWNTs. The nanowires show satisfactory photoluminescence characteristics similar to those of bulk GaN. The noncarbon nanowires and nanotubes have potential applications. For example, GaN nanowires, suitably doped, can have uses in nanoelectronics and in optical devices. BN nanotubes and Si_3N_4 nanowires are useful ceramic materials.

PROPERTIES

Field emission properties of carbon nanotubes have direct applications in vacuum microelectronic devices [38–41]. We have found that carbon nanotubes produced by the pyrolysis of ferrocene on a pointed tungsten tip exhibit high emission current densities with good performance characteristics [42]. The applied voltage was 4.3 kV for a total current of 1 μA and 16.5 kV for 1000 μA. The Fowler–Nordheim (F–N) plot has two distinct regions. The behavior is metal-like in the low field region, while it saturates at higher fields as the voltage is increased. We have obtained a field emission current density of 1.5 A cm^{-2} at a field of 290 V/mm, a value considerably higher than that found with planar cathodes. Accordingly, the field enhancement factor, calculated from the slope of the F–N plot in the low field region is also large. The field emission micrographs reveal the lobe structure symmetries typical of carbon nanotube bundles. The emission current is remarkably stable over an operating period of more than 3 h for various current values in the 10–500 mA range. Carbon nanotubes are considered to be good hosts for hydrogen storage, although there is some controversy about the magnitude of the hydrogen uptake [30,43]. High-pressure adsorption experiments we carried out show that the storage capacity of compact aligned nanotubes prepared by the pyrolysis of ferrocene–hydrocarbon mixtures is between 3 and 4 wt % (143 bar, 27 °C). Electrochemical hydrogen storage in these nanotubes is also substantial [44]. Electrodes made out of aligned MWNTs clearly demonstrate higher electrochemical charging capacities up to 1100 mAh g^{-1}, which correspond to a hydrogen storage capacity of 3.75 wt %. SWNTs and MWNTs (arc-generated), however, show capacity in the range of 2–3 wt %.

ACKNOWLEDGMENTS

The authors thank the Department of Science and Technology, Government of India, and the DRDO (India) for supporting this research. They acknowledge productive collaboration with Dr. B. C. Satishkumar, Dr. R. Sen, Mr. F. L. Deepak, and Mr. G. Gundiah.

REFERENCES

1. S. Iijima. *Nature* **354**, 56 (1991).
2. M. Jose-Yacaman, M. Miki-Yoshida, L. Rendon, T. G. Santiesteban. *Appl. Phys. Lett.* **62**, 202 (1993).
3. V. Ivanov, J. B. Nagy, Ph. Lambin, A. Lucas, X. B. Zhang, X. F. Zhang, D. Bernaerts, G. Van Tendeloo, S. Amelinckx, J. Van Landuyt. *Chem. Phys. Lett.* **223**, 329 (1994).

4. K. Hernadi, A. Fonseca, J. B. Nagy, D. Bernaerts, J. Riga, A. Lucas. *Synth. Met.* **77**, 31 (1996).
5. N. M. Rodriguez. *J. Mater. Res.* **8**, 3233 (1993).
6. R. Sen, A. Govindaraj, C. N. R. Rao. *Chem. Phys. Lett.* **267**, 276 (1997).
7. R. Sen, A. Govindaraj, C. N. R. Rao. *Chem. Mater.* **9**, 2078 (1997).
8. M. Yudasaka, R. Kikuchi, Y. Ohki, S. Yoshimura. *Carbon* **35**, 195 (1997).
9. S. Fan, M. C. Chapline, N. R. Franklin, T. W. Tombler, A. M. Cassel, H. Dai. *Science* **283**, 512 (1999).
10. C. N. R. Rao, A. Govindaraj, R. Sen, B. C. Satishkumar. *Mater. Res. Innov.* **2**, 128 (1998).
11. B. C. Satishkumar, A. Govindaraj, R. Sen, C. N. R. Rao. *Chem. Phys. Lett.* **293**, 47 (1998).
12. S. Seraphin and D. Zhou. *Appl. Phys. Lett.* **64**, 2087 (1994).
13. H. M. Cheng, F. Li, G. Su, H. Y. Pan, L. L. He, X. Sun, M. S. Dresselhaus. *Appl. Phys. Lett.* **72**, 3282 (1998).
14. W. A. de Heer, J. M. Bonard, K. Fauth, A. Chatelain, L. Forro, D. Ugarte. *Adv. Mater.* **9**, 87 (1997).
15. B. C. Satishkumar, A. Govindaraj, C. N. R. Rao. *Chem. Phys. Lett.* **307**, 158 (1999).
16. C. N. R. Rao, R. Sen, B. C. Satishkumar, A. Govindaraj. *Chem. Commun.* 1525 (1998).
17. Z. W. Pan, S. S. Xie, B. H. Chang, L. F. Sun, W. Y. Zhou, G. Wang. *Chem. Phys. Lett.* **299**, 97 (1999).
18. L. Chico, V. H. Crespi, L. X. Benedict, S. G. Louie, M. L. Cohen. *Phys. Rev. Lett.* **76**, 971 (1996).
19. L. Kouwenhoven. *Science* **275**, 1896 (1997).
20. P. L. McEuen. *Nature (London)* **393**, 15 (1998).
21. M. Menon and D. Srivastava. *Phys. Rev. Lett.* **79**, 4453 (1997).
22. M. Menon and D. Srivastava. *J. Mater. Res.* **13**, 2357 (1998).
23. M. S. Fuhrer, J. Nygard, L. Shih, M. Forero, Y. G. Yoon, M. S. C. Mazzoni, H. J. Choi, J. Ihm, S. G. Louie, A. Zettl, P. L. McEuen. *Science* **288**, 494 (2000).
24. J. Li, C. Papadopoulos, J. Xu. *Nature (London)* **402**, 253 (1999).
25. B. C. Satishkumar, P. J. Thomas, A. Govindaraj, C. N. R. Rao. *Appl. Phys. Lett.* **77**, 2530 (2000).
26. F. L. Deepak, A. Govindaraj, C. N. R. Rao. *Chem. Phys. Lett.* **345**, 5 (2001).
27. S. J. Tans, A. R. M. Verschueren, C. Dekker. *Nature (London)* **393**, 49 (1998).
28. R. Martel, T. Schmidt, H. R. Shea, T. Hertel, Ph. Avouris. *Appl. Phys. Lett.* **73**, 2447 (1998).
29. Z. Yao, H. W. Ch. Postma, L. Balents, C. Dekker. *Nature (London)* **402**, 273 (1999).
30. C. N. R. Rao, B. C. Satishkumar, A. Govindaraj, M. Nath. *Chem. Phys. Chem.* **2**, 78 (2001).
31. A. M. Morales and C. M. Leiber. *Science* **279**, 208 (1998).
32. Y. Zhang, K. Suenaga, C. Colliex, S. Iijima. *Science* **281**, 973 (1998).
33. W. Han, S. Fan, Q. Li, B. Gu, X. Zhang, D. Yu. *Appl. Phys. Lett.* **71**, 2271 (1997).
34. M. J. Wang and H. Wada. *J. Mater. Sci*. **25**, 1690 (1990); X. C. Wu, W. H. Song, B. Zhao, W. D. Huang, M. H. Pu, Y. P. Sun, J. J. Du. *Solid State Commun.* **115**, 683 (2000).
35. G. Gundiah, G. V. Madhav, A. Govindaraj, C. N. R. Rao *J. Mater. Chem.* **12**, 1606 (2002).
36. F. L. Deepak, K. Mukhopadhyay, C. P. Vinod, A. Govindaraj, C. N. R. Rao. *Chem. Phys. Lett.* **353**, 345 (2001).
37. F. L. Deepak, A. Govindaraj, C. N. R. Rao. *J. Nanosci. Nanotechnol.* **1**, 303 (2001).
38. W. A. de Heer, A. Chatelain, D. Ugarte. *Science* **270**, 1179 (1995).
39. Q. H. Wang, T. D. Corrigan, J. Y. Dai, R. P. H. Chang, A. R. Krauss. *Appl. Phys. Lett.* **70**, 3308 (1997).
40. J.-M. Bonard, F. Maier, T. Stockli, A. Chatelain, W. A. de Heer, J.-P. Salvetat, L. Ferro. *Ultramicroscopy* **73**, 7 (1998).
41. Y. Saito, K. Hamaguchi, K. Hata, K. Tohji, A. Kasuya, Y. Nishina, K. Uchida, Y. Tasaka, F. Ikazaki, M. Yumura. *Ultramicroscopy* **73**, 1 (1998).
42. R. B. Sharma, V. N. Tondare, D. S. Joag, A. Govindaraj, C. N. R. Rao. *Chem. Phys. Lett.* **344**, 283 (2001).

43. M. S. Dresselhaus, K. A. Williams, P. C. Eklund. *MRS Bulletin* **24**, 45 (1999).
44. G. Gundiah, N. Rajalakshmi, K. S. Dhathathreyan, A. Govindaraj, C. N. R. Rao. *J. Mater. Chem.* (2002). Submitted for publication.